PL-TR-91-3001 AD:

AD-A235 257

Final Report
for the period
June 1990 to
January 1991

The Effects of Space Debris on Solar Propulsion

March 1991

Author:
Mark Skibinski

Approved for Public Release

Distribution is unlimited. The OL-AC PL Technical Services Office has reviewed this report and it is releaseable to the National Technical Information Service, where it will be available to the general public, including foreign nationals.

Phillips Laboratory
Air Force Systems Command
Edwards AFB CA 93523-5000

NOTICE

FOREWORD

This interim report was submitted on completion of this task of JON: 305500R7 by the OL–AC PL/RKAS Branch, at the Phillips Laboratory (AFSC) (formerly Astronautics Laboratory), Edwards AFB CA 93523–5000. OL–AC PL Project Manager was Lt Tim Lawrence.

This report has been reviewed and is approved for release and distribution in accordance with the distribution statement on the cover and on the DD Form 1473.

TIMOTHY J. LAWRENCE, Lt, USAF
Project Manager

BERNARD R. BORNHORST
Chief, Space Propulsion Branch

PETER A. VAN SPLINTER
Director
Applications Engineering Division

SECURITY CLASSIFICATION OF THIS PAGE

REPORT DOCUMENTATION PAGE

Form Approved OMB No 0704-0188

1a REPORT SECURITY CLASSIFICATION UNCLASSIFIED	1b RESTRICTIVE MARKINGS
2a. SECURITY CLASSIFICATION AUTHORITY	3 DISTRIBUTION/AVAILABILITY OF REPORT Approved for Public Release; Distribution is Unlimited
2b DECLASSIFICATION/DOWNGRADING SCHEDULE	
4. PERFORMING ORGANIZATION REPORT NUMBER(S) PL-TR-91-3001	5 MONITORING ORGANIZATION REPORT NUMBER(S)
6a NAME OF PERFORMING ORGANIZATION Phillips Laboratory (AFSC) 6b OFFICE SYMBOL (If applicable) RKAS	7a NAME OF MONITORING ORGANIZATION
6c. ADDRESS (City, State, and ZIP Code) OL-AC PL/RKAS Edwards AFB CA 93523-5000	7b. ADDRESS (City, State, and ZIP Code)
8a NAME OF FUNDING/SPONSORING ORGANIZATION 8b OFFICE SYMBOL (If applicable)	9 PROCUREMENT INSTRUMENT IDENTIFICATION NUMBER
8c. ADDRESS (City, State, and ZIP Code)	10 SOURCE OF FUNDING NUMBERS PROGRAM ELEMENT NO: 62302F PROJECT NO: 3056 TASK NO: 00R7 WORK UNIT ACCESSION NO:

11 TITLE (Include Security Classification)
The Effects of Space Debris on Solar Propulsion (U)

12 PERSONAL AUTHOR(S)
Skibinski, Mark

13a. TYPE OF REPORT	13b TIME COVERED	14. DATE OF REPORT (Year, Month, Day)	15 PAGE COUNT
Final	FROM 9006 TO 9007	9103	36

16 SUPPLEMENTARY NOTATION
OL-AC PL was formerly known as the Astronautics Laboratory (AFSC)

17 COSATI CODES			18 SUBJECT TERMS (Continue on reverse if necessary and identify by block number)
FIELD	GROUP	SUB-GROUP	Mission analysis, orbital debris, solar propulsion
10	01		

19 ABSTRACT (Continue on reverse if necessary and identify by block number)

The objective of this research was to determine the impact of space debris on solar propulsion for orbital transfer missions from Low Earch Orbit (LEO) to Geosynchronous Earth Orbit (GEO). Orbital debris is a major concern because the present solar propulsion development calls for two 40 x 30 meter inflatable concentrators which present a large area for space debris impact. The initial questions to be researched were: 1) How much extra inflationary gas will be required to make up for meteoroid and artificial space debris leaks? and 2) What is the probability of a catastrophic collision with the concentrators? Numerous debris models and many assumptions were used to calculate answers for these questions, but overall the inflatable reflectors were judged to be a plausible concept. It is plausible in that the amount of helium inflatent needed to keep the concentrators rigid is an acceptable weight (12 lbm). Also the probability of a catastrophic collision for a 40 day mission is minimal (0.1%). Further in-depth research and computer simulation is needed to better define the man-made debris distribution for elliptical (transfer) orbits due to their constant changing altitude.

20 DISTRIBUTION/AVAILABILITY OF ABSTRACT ☒ UNCLASSIFIED/UNLIMITED ☐ SAME AS RPT ☐ DTIC USERS	21 ABSTRACT SECURITY CLASSIFICATION UNCLASSIFIED
22a NAME OF RESPONSIBLE INDIVIDUAL Lt Timothy Lawrence	22b TELEPHONE (Include Area Code) (805) 275-5646 22c OFFICE SYMBOL OL-AC PL/RKAS

DD Form 1473, JUN 86 — Previous editions are obsolete — SECURITY CLASSIFICATION OF THIS PAGE

TABLE OF CONTENTS

LIST OF FIGURES

LIST OF TABLES

INTRODUCTION

Solar Propulsion Concept

For the solar propulsion concept (SPC) there are two energy focusing concentrators integrated with a solar flux-absorbing thruster and a single fuel tank. This solar powered propulsion system can make Low Earth Orbit (LEO) to Geosynchronous Earth Orbit (GEO) missions more profitable. The SPC will double the Isp of conventional orbital transfer vehicles (1000 sec for a hydrogen working fluid at 3000 K), and consequently double the payload moved to GEO with half the propellant used by current systems.

Two large solar concentrators gather, focus, and concentrate approximately 1500 kW into their respective thruster cavities to produce the required energy to heat the working fluid (hydrogen) to 3000 Kelvin to produce thrust. Note that for the calculations in this paper hydrogen is the working fluid for the thrusters and helium, the inflatant for the concentrators. See Figure 1.

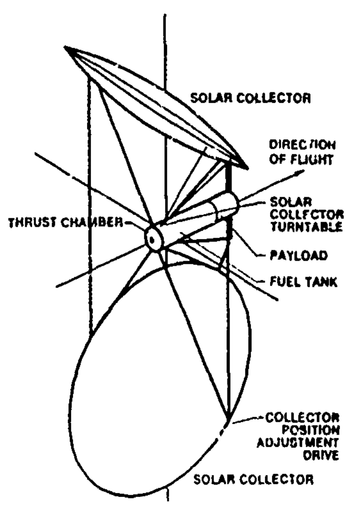

ENGINES		
Thrust (2)	50 Lbf	
Maximum Acceleration	0.002 G's	
Minimum Acceleration	0.001 G's	
Engines, Absorbers		422 Lbm
Attitude Control System		90 Lbm
REFLECTORS		
Minor Diameter	100 Ft	
Major Diameter	135 Ft	
Turnables		61 Lbm
Truss Joints		19 Lbm
Torus Components		90 Lbm
Pressurization & Feed System		34 Lbm
Paraboloid Components		316 Lbm
Truss Tubes		58 Lbm
PROPELLANT/TANK		
Fuel Tank Structure (Empty)		1,950 Lbm
Fuel		20,610 Lbm
Avionics		350 Lbm
PAYLOAD		
Payload to GEO		26,000 Lbm
LEO Initial Weight		50,000 Lbm
LEO-GEO Transfer Time	30 Days	

Figure 1. Solar Propulsion System

The two inflatable concentrators are the focus of our concern about orbital debris flux. The SPC's two off-axis parabolic concentrators are designed to have an approximate 40-meter major diameter by 30-meter minor diameter to cover the projected sun diameter. The concentrators are pressurized double concavo-convex lenses that have a hollow interior and a thin film skin. Each concentrator looks like a giant clam shell (Fig. 1) with an approximate projected area of 100 square meters (Ref. 1, p. 3).

The thruster is a dual cavity, dual nozzle device designed to capture the solar energy from both collectors. The single working fluid is heated and expanded indirectly by conductive heating from a solar heated material in the cavity atmosphere. Without igniting the fluid, thrust is produced in the propulsive nozzle and the gas expelled. Table 1 defines some of the solar propulsion parameters (Ref. 1, p. 2-3).

Table 1. Solar Propulsion Parameters
Thrust = 100.0 lbf
Isp = 1000 sec (Hydrogen @ 3000 K)
Gross weight (to LEO) = 50,000 lbm
Reflector projected area = 1000 m2
Volume inside both reflectors = 175,000 ft3
Required pressure in reflectors = 2.46 X 10-4 psi
Delivery weight (to GEO) = 28,000 lbm
Estimated trip time = 30 days

DEBRIS ISSUES

To clarify the complexity of the problem, it is necessary to provide some basic definitions and explanations. This paper addresses two types of space debris hazards: meteoroids and orbital debris.

Natural meteoroids are a natural space debris hazard that is not usually present in an earth orbit. Meteoroids come from a variety of possible sources including asteroids, comets, and the moon. Meteoroids do not enter an Earth orbit because they remain in a orbit similar to that of their parent body.

Artificial (orbital) space debris is man-made material orbiting the earth. Large pieces of artificial debris include spent rocket stages, nonoperational payloads, payload separation hardware, and satellite breakup fragments (Ref. 2, p. 1). Micro-size objects consist of paint particles from spacecraft surfaces, aluminum oxide and other propellant particles or droplets. Figure 2 breaks down the percentage of debris in each of the categories.

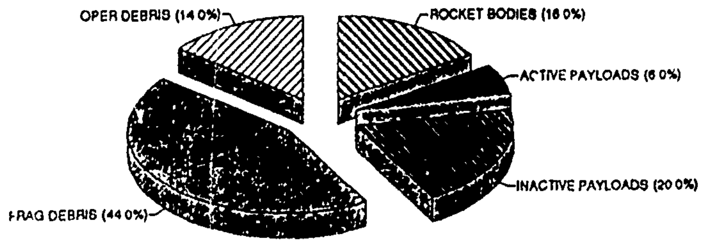

Figure 2. On-Orbit Population (Ref. 3, p. 5)

In general, natural meteoroids have greater relative velocities (20 km/s) than orbital debris (10 km/s)(Ref. 4, p. 4). At any one time there are 200 kg of meteoroids within 2000 km of the earth's surface. Most of these particles have an average 1-mm diameter. The flux of natural meteoroids varies in time with the sun's solar activity cycles (Ref. 4, p. 1).

On the other hand, there is 3,000,000 kg of orbital debris within the same 2000-km altitude band. Over 7,000 objects presently tracked by NORAD comprise most of this orbital debris mass (Ref. 4, p. 4). These mass distributions can be deceiving because there is another 3.5 million man-made fragments orbiting the earth whose mass is only about 1000 kg of that total (Table 2) This means that of the 3.535 million man-made objects orbiting the earth in LEO, only 7,000 (0.2%) are tracked by NORAD. NORAD presently has the capability of tracking particles that are 10 cm or greater in diameter (Ref. 4, p. 3-4).

Particles with diameters between 1 cm and 10 cm comprise another 0.5% of this 3.525 million population. Powerful optical telescopes (like MIT's ground telescopes) can track particles with diameters as small as 1 cm on a nonoperational basis.

The remaining 99.3% of these 3.525 million man-made objects in LEO have diameters of less than 1 cm (Ref. 4, p. 4). Although current ground-based sensors can not track these objects, flux and probability curves are generated by extrapolations and impact data taken from recovered satellites and space vehicles. Table 2 shows the orbital debris population and percentages by diameter and mass.

Table 2. Estimated Artificial Debris Propulsion (Ref. 4, p. 4)

Size	No. of Objects	Percentage	Mass (kg)	% Mass
> 10 cm	7,000	0.2	2,999,000	99.97
1-10 cm	17,000	0.5	1,000	0.03
< 1 cm	3,500,000	99.3	————	———
TOTALS	3,524,500	100.0	3,000,000	100.00

There is a small size range in which the number of meteoroids is significantly larger than the number of man-made debris. At present meteoroid populations are significantly higher in the 0.1 to 1-mm diameter range. Some predictions show that man-made debris will outnumber meteoroids in this size range around the turn of the century (Ref. 4, p. 15-16).

The large numbers of nontrackable debris makes calculating debris flux on the concentrators a dilemma. Although debris particle diameters seem small, their extremely high relative velocities in LEO (average 10 km/s) give them large kinetic energies. For instance, impact with a typical 3-mm particle in space is analogous to impact with a bowling ball at 60 miles per hour. Impact with a 1-cm particle has the same kinetic energy as impact with a 400-lb security safe at 60 miles per hour (Fig. 3). Thus it is obvious that the problem of tiny orbiting particles impacting a thin-film, inflatable solar concentrator is not trivial.

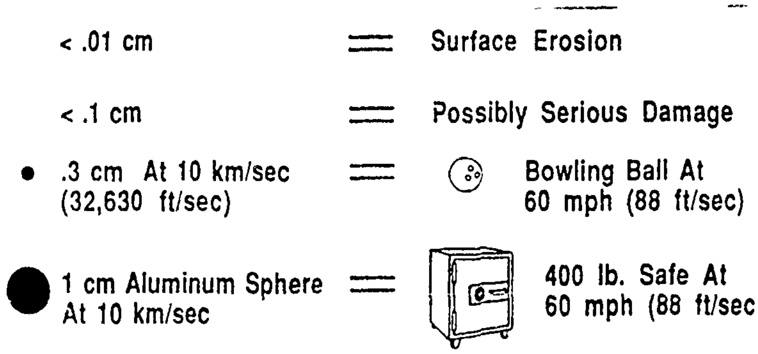

Figure 3. Kinetic Energy of Space Debris

Certain areas around the earth have higher orbital debris densities than others. Debris densities are highly dependent on altitude and inclination. Other orbital elements such as line of nodes and eccentricity are similar and average out (Ref. 5, p. 18).

Highest debris density occurs in the 2,000-km altitude band. Within this band distinct peaks occur at altitudes of 800 km and 1400 km (Fig. 4)(Ref. 6, p. 3-4). Notice that in Figure 5 the spatial densities of orbital debris drop off considerably from 1500 km to GEO.

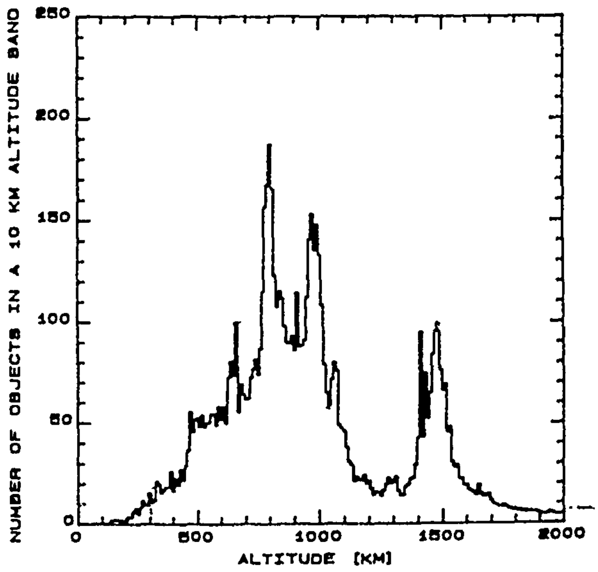

Figure 4. Altitude Distribution of Trackable Debris (Ref. 4, p. 4)

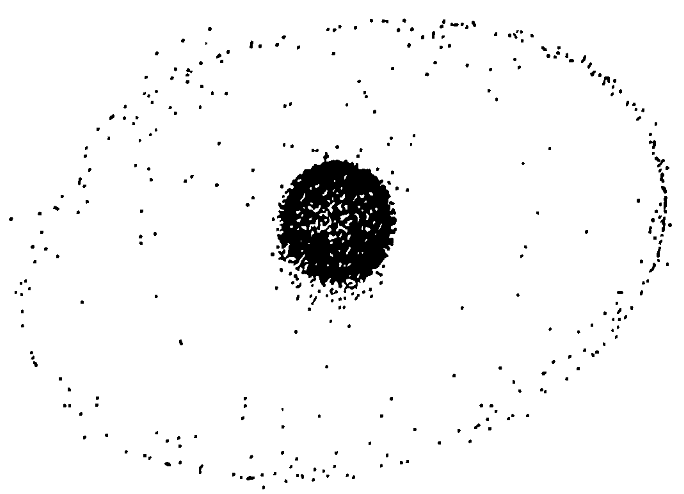

Figure 5. Overall Earth Orbit Distribution (Ref. 6, p. 12)

Debris densities are also greater at higher inclinations because space activity is more prevalent in these areas. As a space vehicles travels along its transfer orbit large amounts of debris are left behind. Peak density inclinations are around 75 deg where there is a critical inclination (63 deg), 82 deg, sunsynchronous orbits (100 deg) and polar orbits (90 deg)(Ref. 5, p. 18).

Most debris particles are in very near circular orbits, with an eccentricity of less than 0.05. A natural circularization of debris orbits is a result of air drag on the particle (Ref. 5, p. 18).

Intentional satellite breakups and explosions are the largest source of debris. Because of the frequency of occurrence, intentional explosions of satellites is the largest source of debris and the practice must be discontinued immediately. "As a result (of an explosion) the fragments initially form an elliptical cloud of shrapnel. Over time the differential orbital parameters of the fragments cause the cloud to dissociate into a torus about the Earth." 1 (See Fig. 6.)

Collisions of two satellites or debris particles at hypervelocity impacts (average 10 km/s) could produce up to 10 times the amount of particles that an explosion creates. These collisions would also complicate the environment because the size of particles expelled is much smaller than that of average explosion particles. Other sources of debris particles are satellite deterioration and operational mission activities.

Current mathematical models consider various traffic patterns and satellite breakups to predict future debris populations. Some theorists feel that these models show that if current launch procedures continue at increased rates, debris collision will become much more prevalent because the population of small size debris could increase 10% per year.

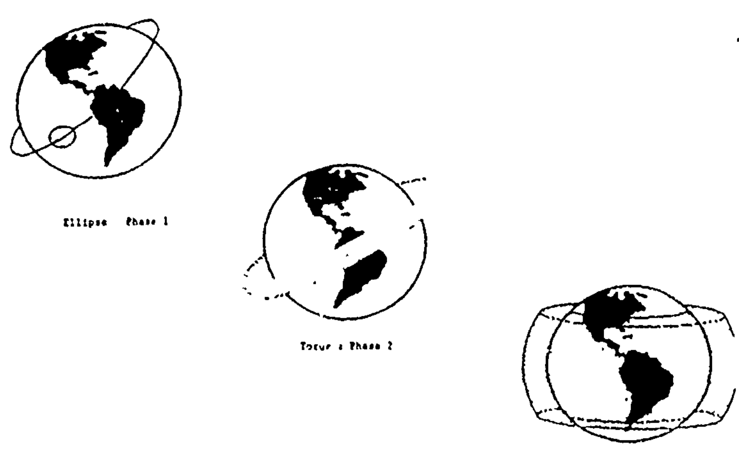

Figure 6. Phases of Debris Cloud Evolution (Ref. 3, p. 2)

A 10% per year increase rate could result in an unstable environment in which a critical particle density is reached and random debris collision approach runaway rates. We could reach this critical density as soon as the mid 21st century and an unstable environment not long after in the late 21st century (Ref. 2, p. 12).

According to Donald J. Kessler (NASA/JSC), "Based on today's launch rates and the natural population decay rate, extrapolated to the year 2000+, there may be a hazardous collision among any two space objects once every 1 to 4 years." (Ref. 5, p. 20)

Calculations modeling space debris flux and collision probabilities are very uncertain. Insufficient data on small particles, unknown levels of future space activities (launch rates), the randomness of our orbital debris cloud, and possible exaggerated debris growth rates.

CONCENTRATOR ISSUES

The effect of meteoroids and orbital debris on the balloon-like concentrators is a major question. To answer this question, we need to consider a number of parameters including: the transfer orbit profile and trip time, the projected area relative to the velocity vector, total time spent in an altitude interval, the material of the concentrator skin, the pressure and volume inside the concentrator, and the amount and size of holes in the concentrator.

The transfer orbit for the SPC is uncertain. Recently the Astronautics Laboratory has performed computer optimizations to determine the best transfer orbit profile. The driving factors were 1000 sec Isp, 50,000 lbm initial weight out of the shuttle bay at LEO, 50 lbf of estimated thrust, and 0.5 thruster efficiency.

Right now a multiple burn Hohlman transfer is the most efficient and practical SPC transfer. The Fortran program called Multiburn was modified to help design a solar propulsion mission (Ref. 7). Multiburn performs a trajectory analysis for multiple burn

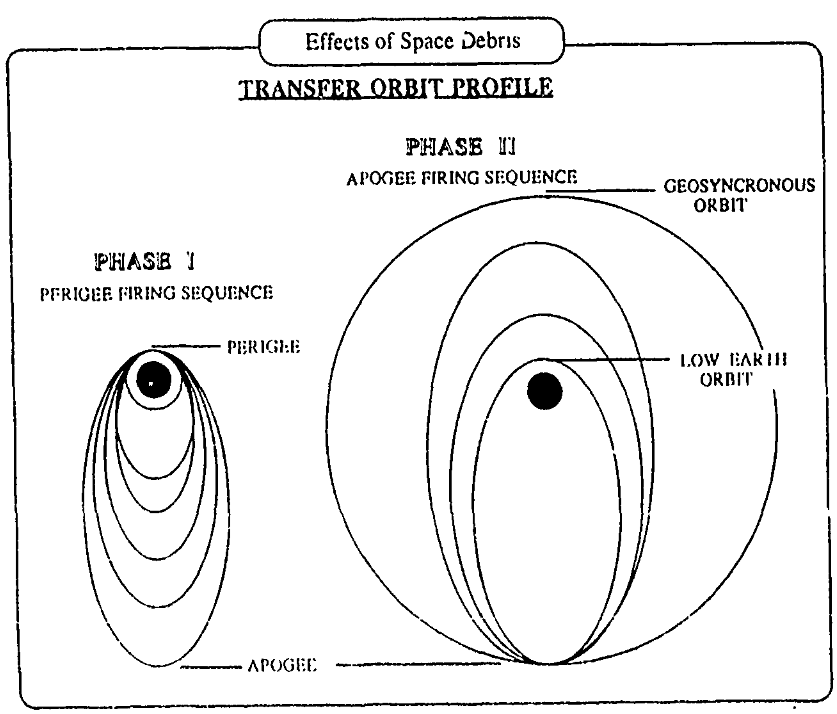

Figure 7. Solar Propulsion Transfer Strategy

transfers. Program results show that numerous perigee burns and a couple of apogee burns produce the best transfer profiles. Modified multiburn results are contained in Appendix A.

Figure 7 illustrates that the strategy of this transfer is to raise the radius of apogee with consecutive perigee burns until a geosynchronous altitude is reached. At this point the SPC is in an elliptical orbit with a perigee altitude of 280 km (approximate) and an apogee altitude of 35,800 km (GEO).

The second phase of the transfer is to raise the perigee altitude out to GEO by performing consecutive apogee burns. The final apogee firing would circularize the transfer at GEO.

Although the complete evaluation and optimization of the number of burns is not yet complete, a ratio of 10 perigee burns to every apogee burn seems a good first assumption. Table 3 shows the number of burns used as a rough approximation in this space debris scenario.

Table 3. SPC Transfer Orbit Profile (Estimated)
Perigee burns = 120
Apogee burns = 12
Approximate trip time = 24.8 days
Projected reflector area = 100 m^2 (each)

The acronym HAIR stands for highly accurate inflatable reflectors. The HAIR is currently the most acceptable concentrator design for the solar propulsion concept. In the mid 1980's the basic concept was designed and developed using thin films to make the inflatable "clam shell" reflectors.

Inflatable concentrators are preferred over other types of rigid concentrators because of their large weight savings to GEO. The HAIR design would yield concentration ratios greater than 10,000:1 to assure that the minimum amount of energy is transferred to the fuel to expand the gas and propel the spacecraft.

In 1986 a firm called L'Garde presented their final report on their development of these inflatable reflectors for the SPC. Using their 1986 results and parameters for all calculations, L'Garde is furthering their design and development of these reflectors.

The material used for the reflective surface of the parabola will be 0.25-mm thick Teflon with vapor deposited aluminum. The internal pressure for inflation and reflectance is 2.46E-04 psi. L'Garde calculates the gas volume for the two collectors to be 175,000 cubic feet (Ref. 8, p. 10-15).

APPROACH TO THE DEFLATION PROBLEM

The focus of the deflation problem is determining the number and size of all the space debris particles that will penetrate the concentrators during a transfer and at what time the particles make the penetration.

Many assumptions had to be made in order to calculate the amount of inflatant lost during a typical SPC mission. These included:

1. Calculate the particle flux at worst case altitude (800 km) as a first cut approximation.

2. Assume a high density inclination.

3. Assume an average 0.5-mm orbital debris diameter for man-made hits based on probabilities.

4. Assume an average 0.2-mm meteoroid diameter for all meteoroid hits based on probabilities.

5. Assume that collisions with particles less than 0.1 mm will not penetrate the concentrators.

6. Assume the flow of helium through the holes is isentropic (frictionless), conservation of mass, and constant density.

7. Assume the particle only creates a hole in one side of the concentrator.

8. Assume that the length of the mission is 36 days or 1/10 of a year.

9. Assume that the area of the holes will be cumulative starting with day 1 and that the total loss of inflatant is exponential with time.

10. Assume that orbital debris growth will be roughly 10% per year.

11. Assume that the diameter of a hole in the concentrator is equal to the diameter of the particle that impacted. (This assumption should be acceptable because the other 10 assumptions are for a worst case scenario.)

To determine the amount of inflatant needed to replace inflatant lost due to space debris leaks requires an estimate of the number and size of particle hits. Flux graphs based on different mathematical models were analyzed to derive an impact rate. Read the flux graphs in Figures 8 and 9 carefully. The graphs are on a logarithmic scale and show impacts per time versus a particle size. The x axis shows a cumulative particle size. The y axis shows flux which is the number of impacts per year on a given surface area. In Figure 8 the flux of a 1-cm particle or greater is 0.4 impacts on a large space structure at an altitude of 500 km and an inclination of 30 degrees. That is approximately one impact every 2.5 years. This would be a catastrophic hit for most small satellites.

Figure 9 is the flux graph used in the Astronautics Laboratory's calculations because it is the worst case altitude and inclination. The spacecraft surface area will be scaled up to 2000 square meters by a factor of 50.

Consequently, the two concentrators can expect an impact with a 2-mm particle or greater (approximately) every year if they were continuously in that worst case orbit fully inflated.

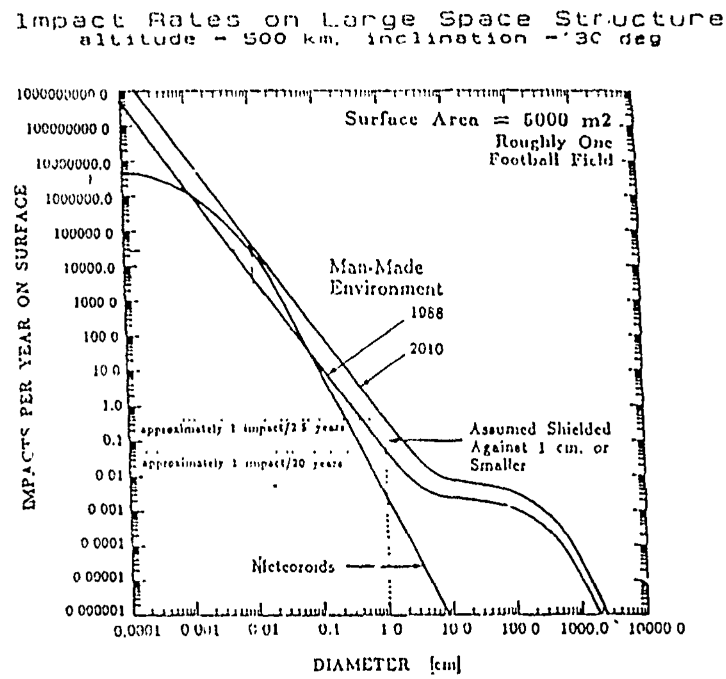

Figure 8. Space Debris Impacts on a Large Class Spacecraft (Ref. 4, p. 15)

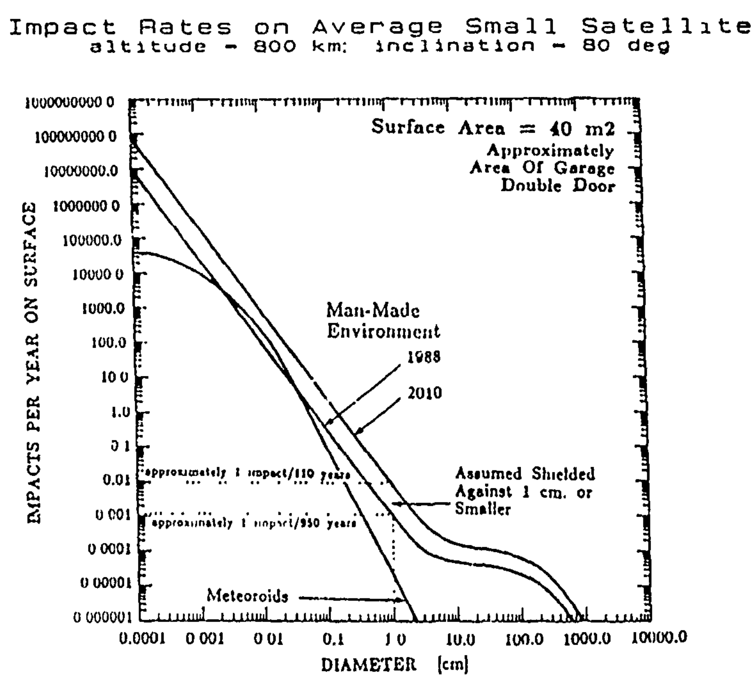

Figure 9. Space Debris Impacts on a Small Spacecraft (Ref. 4, p. 16)

To calculate an average mission flux consider the meteoroid and man-made debris separately. Figure 8 shows the meteoroid flux at the 0.01-cm (0.1-mm) mark to be 200 impacts per year. To scale up the reflectors' surface area multiply by a factor of 50. Then the flux works out to 10,000 hits per year.

There are two rates for man-made debris: the current rate and a predicted future date. The 1988 flux rate of 100 impacts per year, when scaled up by a factor of 50, becomes 5,000 impacts per year. Given a 10% annual increase in population, the predicted flux for the year 2010 is 900 impacts per year. Scaled up for a 2,000 square meter area, the rate becomes 45,000 impacts per year (Ref. 4, p. 15-16). Table 4 summarizes the impact rate calculations.

Table 4. Impact Rates for Two (1000 m^2) Concentrations

Year	Debris Type	Impacts/Year
1988	Man-made	5,000
2010	Man-made	45,000
1988	Meteoroid	10,000
2010	Meteoroid	10,000
** Impacts are for 0.1 mm and greater particles		

Next, using the previous impact rate calculation, we must calculate the area of the hole produced by an average size impact. Since our man-made and natural debris average diameters are 0.5 mm and 0.2 mm, respectively, the area for a single particle hit is assumed to be :

Man-Made Particles 0.5 mm	1.9635 x 10-3 cm
Natural Meteoroid 0.2 mm	3.1416 x 10-4 cm

The conservation of mass flow (i.e., in a rocket engine when the mass of the escaping gas equals the mass created by burning the fuel) and constant density were assumed. The following procedure was used to calculate the inflatant lost:

$$A1 * V1 = A2 * V2$$

For very small openings escape velocity of the inflatant is (Ref. 9, p. 239):

$$V2 = [\, 2(P1-P2) / \text{Density}]^{1/2}$$

Calculate density of helium at 2.46E-04 psi and 277.8 Kelvin.

$$\text{Density} = 2.9304 \times 10^{-9}\ g/cm^3$$

Calculate the gas's escape velocity:

$$V2 = 1076\ m/sec\ (\text{Assume } P2 = 0\ psi)$$

Calculate an inflatant loss rate: A2*V2*Density lbs / (day*hit).

Man-Made loss rate = 1.1795×10^{-4} lbs/(hit day)

Natural loss rate = 1.8872×10^{-5} lbs/(hit day)

Calculate a Hit*Day factor for a 40-day mission:

a) Divide the number of Hits/year by 365.

b) Multiply that number by 40 days for a linear relationship.

c) Calculate an area under the curve by multiplying b) by 40 days again and divide by 2.

Man-Made = (123*40*40/2) = 98,400 Hit*Day

Natural = (27.4*40*40/2) = 21,920 Hit*Day

To find the total amount of extra inflatant needed, multiply loss rate by Hit*Day factor to get lbs of gas required to keep reflectors inflated for 40 day mission. A summary of these results are in Table 5.

Table 5. Inflatant Needed to Compensate for Debris Leaks

Man-made	11.61 lbs
Natural	0.41 lbs
Total	12.02 lbs of helium

Compared with the L'Garde results, 12.02 lbs of helium to compensate for debris leaks is much lower. The problem with this result is not the method of analysis but the assumption of an average particle size. A better approach would be to obtain a sample. Base distribution on the probabilities of particle impact, simulate hits for a variety of particle sizes, and calculate the losses as time goes on.

Performing this type of calculation becomes very time consuming. It would be much easier for a computer program to perform the calculations. Future modifications to the Multiburn program will incorporate this approach and yield more accurate numbers.

The real value of this investigation into the inflation problem is the discovery of its vast complexities. Further research is needed to see if a inflatable concentrator is truly realistic.

Remaining Issues

The problem with calculating impacts on a reflector which is in an elliptical transfer orbit has not yet been addressed. The calculations were performed assuming a circular orbit at a constant altitude. A relatively short computer program could integrate these changing parameters for noncircular orbits and then calculate particle impacts and deflation rates.

Also the position of the concentrators into low profiles or low projected areas with respect to the direction of flight can result in a significantly smaller number of hits.

Although the amount of inflatant turned out to be relatively low, the errors and assumptions identified the fact that different dependent and independent variables need to be considered. Further development of computer calculations for elliptical transfer orbits and development of the impact calculation for various sized particles will result in a more accurate inflatant weight determination.

CATASTROPHIC COLLISION PROBABILITY

Calculating the probability of a catastrophic impact with a piece of trackable debris is important in determining the feasibility of the system. Because the concentrators have such a large surface area, the risk of collision is greater than it is for an average satellite mission.

One possible approach for this calculation makes use of the kinetic theory of gases. The modified Multiburn program performs many iterations to calculate the total amount of time the spacecraft spends in an altitude interval after several elliptical transfer orbits. (See Appendix B.) Applying the kinetic theory of gases, Multiburn calculates probabilities using the total amount of time spent in a certain spatial density.

Applying this theory to a typical solar propulsion mission, the probability of collision with a piece of orbital debris in low earth orbit can be calculated. This probability is a function of: 1) relative velocity between the spacecraft and orbital debris; 2) the projected cross sectional area of the spacecraft; 3) spatial density of debris traveled through and 4) the time spent passing through that volume. Figure 10 below illustrates the probability of collision (Ref. 3, p. 3).

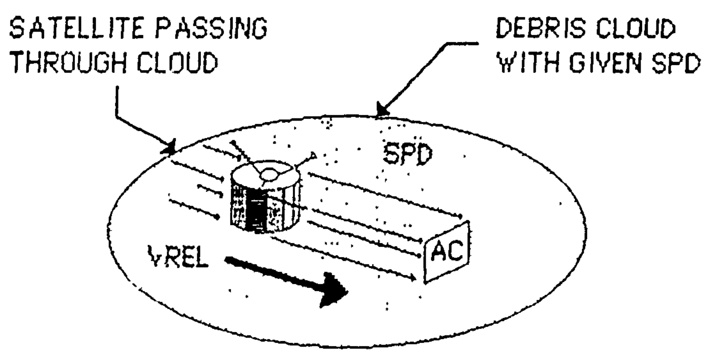

Figure 10. Probability of Collision

Spatial density (SPD) is a mean population density as a function of altitude and the amount of debris in a given volume band. The SPD term is calculated by finding the average number of objects located within 50 km wide concentric volume shells.

The probability equation from Reference 10, p. 3 is:

$$PC = 1 - \exp[-(SPD * AC * Vral - TCP)]$$

** if PC is small, then PC = (SPD * AC *Vrel * TOP)
PC = probability of collision

AC = cross-sectional area of spacecraft (km^2)
SPD = number of objects per cubic km
Vrel = relative velocity between satellite and debris
TOP = time of passage (sec)

A first attempt at analyzing the SPC transfer orbit used time intervals (TOP) of one year in each altitude band. Since the space shuttle is to deliver the SPC at approximately 280 km, the first probability uses the highest spatial density in a 200-km altitude interval starting at an altitude of 200 km. The last probability is at 2400 km because the spatial density becomes so small that the probability of collision is negligible. Table 6 lists the catastrophic collision probabilities.

The problem with using one year time intervals is that a SPC mission is only 40 days. Also as previously mentioned the series of perigee and apogee burns are elliptical transfer orbits that are constantly changing in altitude over time. The modified Multiburn computer program adds up the total time spent in each 200-km altitude band. Results of these total times at an altitude interval are contained in Appendix B. Results reveal that the longest time spent in a single altitude band (200–400 km) is about one day (assuming 120 perigee burns and 12 apogee burns). Table 6 also shows the probabilities of collision for one day at each interval.

The other data used in the probability calculation is:

Vrel = 10 km/sec

AC = 2,000 m^2

SPD = See Appendix C (Ref. 10)

Table 6. Catastrophic Collision Probabilities

Altitude (km)	SPD (No. objects/km^2)	1 year Probability	1 day Probability
200-400	0.16051E-08	0.001	0.000003
400-600	0.56945E-08	0.030	0.000082
600-800	0.13564E-07	0.086	0.00023
800-1000	0.15585E-07	0.098	0.00077
1000-1200	0.89068E-08	0.056	0.00015
1200-1400	0.24093E-08	0.015	0.000042
1400-1600	0.95707E-08	0.060	0.00017
1600-1800	0.25119E-08	0.016	0.000043
1800-2000	0.74911E-09	0.0047	0.000013
2000-2200	0.51456E-09	0.0033	0.000009
2200-2400	0.21176E-09	0.0013	0.000004

The results from Table 6 clearly show that for a 30–40 day transfer orbit, the chance of colliding with a piece of trackable debris is 0.1 percent at the highest density altitude (800 km). As an unrealistic overestimation of one orbiting at 800 km give us 9.8 percent chance of catastrophic collision. Even though these probabilities are very small, the approach and the computer code will be beneficial in the future as the space debris population grows.

Debris Contour Maps

An interesting idea developed during this research program was artificail debris contour plots for future orbit and mission designers. these maps take existing data such as altitude /population distributions and inclination/population distributions and combine them into one color coded contour plot. This maps would show high risk areas as a function of altitude and inclination. High risk contour plots of debris would allow astronautical engineers and orbit designers to avoid high density areas if possible. Sample plots are contained in Appendix D. The data to generate these plots was limited and the program was not able to extrapolate to get even contours but the idea could be useful in the future.

REFERENCES

1. Laug, K., "The Solar Propulsion Concept is Alive and Well at The Astronautics Laboratory," Edwards AFB CA, 1990.

2. Johnson, N.L. and McKnight, D.S., Artificial Space Debris, Orbit Book Company, Inc., Maletar FL, 1987.

3. McKnight, D.S., "Space Debris For Lawyers," Prepared for the American Bar Assoc. Annual Meeting Toronto Canada, 4-11 August 1988.

4. Interagency Group (IG) (Space) for National Security Council "Report on Orbital Debris," Washington D.C., February 1988

5. European Space Agency, A Report From: "Space Debris," ISSN 079-6566, Paris, France, 1988.

6. Stein, B., "Environmental and Materials Effects," NASA N89-23529.

7. Redding, D.C., Multiburn Fortran program using the results from "Highly Efficient, Very Low Thrust Transfer to GEO: Exact and Approximate Solutions," AIAA-62-1484, San Diego CA, 1982.

8. Veal, G.R., "Highly Accurate Inflatable Reflectors, Phase II," AFRPL-TR-86-089, L'Garde, Inc., Tustin CA. March 1987.

9. Halliday, D., Fundamentals of Physics. John Wiley & Sons, Inc. New York, 1974.

10. McKnight, D.S., "Breakups and Their Effect on the Catalog Population," AIAA/NASA/DOD Orbital Debris Conference, Baltimore MD., April 16-19, 1990. AIAA 90-1358.

Kessler, D.J., "Orbital Debris Environment for Spacecraft Designed to Operate in Low Earth Orbit," NASA Tech. Memo: 100 471, April 1989.

Nahra, H.K., "Effect of Micrometeoroid and Space Debris Impacts on the Space Station Freedom Solar Array Surfaces." NASA Tech. Memo, 102287, San Diego CA. April 24-29, 1989.

APPENDIX A

MULTIBURN TRANSFER ORBIT RESULTS

PERIGEE BURNS

BURN NUMBER	MASS RATIO	DELV BURN	DELV TOT	THIS TIME	TOTAL TIME	PROP BURN
1	.9980289	67.08	67.08	1.5124	1.5124	98.557
2	.9980288	67.08	134.16	1.5238	3.0362	98.367
3	.9980287	67.09	201.25	1.5354	4.5715	98.179
4	.9980285	67.09	268.34	1.5471	6.1186	97.993
5	.9980283	67.10	335.44	1.5591	7.6777	97.810
6	.9980280	67.11	402.55	1.5712	9.2489	97.630
7	.9980277	67.12	469.67	1.5835	10.8324	97.453
8	.9980274	67.13	536.80	1.5960	12.4284	97.278
9	.9980270	67.14	603.94	1.6087	14.0371	97.106
10	.9980265	67.16	671.10	1.6216	15.6587	96.936
11	.9980260	67.18	738.28	1.6347	17.2934	96.769
12	.9980255	67.19	805.47	1.6481	18.9415	96.605
13	.9980249	67.21	872.69	1.6616	20.6031	96.443
14	.9980243	67.24	939.92	1.6754	22.2785	96.283
15	.9980236	67.26	1007.18	1.6894	23.9680	96.126
16	.9980228	67.28	1074.47	1.7037	25.6716	95.972
17	.9980221	67.31	1141.78	1.7181	27.3898	95.820
18	.9980212	67.34	1209.12	1.7329	29.1226	95.670
19	.9980204	67.37	1276.48	1.7479	30.8705	95.523
20	.9980195	67.40	1343.88	1.7631	32.6336	95.378
21	.9980185	67.43	1411.32	1.7786	34.4122	95.235
22	.9980175	67.47	1478.78	1.7944	36.2067	95.095
23	.9980164	67.50	1546.29	1.8105	38.0172	94.957
24	.9980153	67.54	1613.83	1.8269	39.8440	94.822
25	.9980142	67.58	1681.41	1.8435	41.6875	94.689
26	.9980130	67.62	1749.03	1.8605	43.5480	94.558
27	.9980117	67.66	1816.70	1.8778	45.4258	94.429
28	.9980104	67.71	1884.40	1.8954	47.3211	94.303
29	.9980091	67.75	1952.16	1.9133	49.2344	94.179
30	.9980077	67.80	2019.96	1.9316	51.1660	94.057
31	.9980062	67.85	2087.81	1.9502	53.1162	93.937
32	.9980048	67.90	2155.71	1.9692	55.0853	93.820
33	.9980032	67.95	2223.66	1.9885	57.0739	93.704
34	.9980017	68.01	2291.67	2.0083	59.0821	93.591
35	.9980000	68.06	2359.73	2.0284	61.1105	93.480
36	.9979984	68.12	2427.85	2.0489	63.1594	93.371
37	.9979966	68.18	2496.03	2.0698	65.2292	93.264
38	.9979949	68.24	2564.26	2.0912	67.3205	93.159
39	.9979931	68.30	2632.56	2.1130	69.4335	93.057
40	.9979912	68.36	2700.92	2.1353	71.5688	92.956
41	.9979893	68.43	2769.35	2.1580	73.7268	92.857
42	.9979873	68.49	2837.85	2.1812	75.9081	92.761
43	.9979853	68.56	2906.41	2.2050	78.1130	92.666
44	.9979833	68.63	2975.04	2.2292	80.3422	92.573
45	.9979812	68.70	3043.74	2.2539	82.5962	92.483
46	.9979790	68.78	3112.52	2.2793	84.8754	92.394
47	.9979769	68.85	3181.37	2.3051	87.1805	92.307
48	.9979746	68.93	3250.30	2.3316	89.5121	92.222
49	.9979723	69.01	3319.30	2.3586	91.8708	92.139
50	.9979700	69.08	3388.39	2.3863	94.2571	92.058
51	.9979676	69.17	3457.55	2.4146	96.6717	91.979
52	.9979652	69.25	3526.80	2.4436	99.1153	91.902
53	.9979627	69.33	3596.14	2.4733	101.5886	91.826
54	.9979602	69.42	3665.55	2.5037	104.0923	91.752
55	.9979576	69.51	3735.06	2.5348	106.6271	91.680
56	.9979550	69.59	3804.65	2.5667	109.1938	91.610
57	.9979524	69.69	3874.34	2.5994	111.7932	91.542

58	.9979497	69.78	3944.12	2.6329	114.4261	91.475
59	.9979469	69.87	4013.99	2.6672	117.0934	91.410
60	.9979441	69.97	4083.96	2.7025	119.7958	91.347
61	.9979413	70.06	4154.02	2.7386	122.5345	91.286
62	.9979384	70.16	4224.18	2.7757	125.3102	91.226
63	.9979354	70.26	4294.45	2.8138	128.1240	91.168
64	.9979324	70.36	4364.81	2.8529	130.9770	91.111
65	.9979294	70.47	4435.28	2.8931	133.8701	91.057
66	.9979263	70.57	4505.85	2.9344	136.8045	91.003
67	.9979232	70.68	4576.53	2.9768	139.7813	90.952
68	.9979200	70.79	4647.32	3.0205	142.8018	90.902
69	.9979168	70.90	4718.22	3.0654	145.8672	90.853
70	.9979135	71.01	4789.23	3.1115	148.9787	90.807
71	.9979102	71.12	4860.35	3.1591	152.1378	90.761
72	.9979068	71.24	4931.59	3.2080	155.3458	90.718
73	.9979034	71.35	5002.94	3.2585	158.6043	90.675
74	.9978999	71.47	5074.41	3.3104	161.9147	90.635
75	.9978964	71.59	5146.01	3.3640	165.2787	90.595
76	.9978929	71.71	5217.72	3.4193	168.6980	90.558
77	.9978893	71.84	5289.55	3.4763	172.1742	90.521
78	.9978856	71.96	5361.51	3.5351	175.7093	90.486
79	.9978819	72.09	5433.60	3.5959	179.3052	90.453
80	.9978782	72.21	5505.81	3.6587	182.9639	90.421
81	.9978744	72.34	5578.15	3.7236	186.6874	90.390
82	.9978705	72.47	5650.63	3.7907	190.4781	90.361
83	.9978667	72.61	5723.23	3.8601	194.3382	90.333
84	.9978627	72.74	5795.97	3.9320	198.2702	90.306
85	.9978588	72.87	5868.85	4.0064	202.2766	90.281
86	.9978547	73.01	5941.86	4.0836	206.3601	90.257
87	.9978507	73.15	6015.01	4.1635	210.5237	90.235
88	.9978465	73.29	6088.30	4.2465	214.7702	90.213
89	.9978424	73.43	6161.73	4.3326	219.1028	90.193
90	.9978381	73.58	6235.31	4.4221	223.5249	90.174
91	.9978339	73.72	6309.03	4.5151	228.0400	90.157
92	.9978296	73.87	6382.90	4.6118	232.6518	90.141
93	.9978252	74.02	6456.92	4.7124	237.3642	90.125
94	.9978208	74.17	6531.09	4.8172	242.1814	90.111
95	.9978164	74.32	6605.40	4.9264	247.1078	90.099
96	.9978119	74.47	6679.88	5.0403	252.1481	90.087
97	.9978073	74.63	6754.50	5.1591	257.3072	90.077
98	.9978027	74.78	6829.29	5.2833	262.5905	90.067
99	.9977981	74.94	6904.23	5.4131	268.0036	90.059
100	.9977934	75.10	6979.33	5.5489	273.5525	90.052
101	.9977887	75.26	7054.59	5.6911	279.2435	90.046
102	.9977839	75.43	7130.02	5.8401	285.0836	90.041
103	.9977791	75.59	7205.61	5.9964	291.0800	90.037
104	.9977742	75.76	7281.36	6.1606	297.2407	90.034
105	.9977693	75.92	7357.28	6.3332	303.5739	90.033
106	.9977643	76.09	7433.38	6.5149	310.0887	90.032
107	.9977593	76.26	7509.64	6.7062	316.7949	90.032
108	.9977542	76.44	7586.08	6.9080	323.7030	90.033
109	.9977491	76.61	7662.69	7.1212	330.8242	90.035
110	.9977440	76.79	7739.47	7.3466	338.1707	90.038
111	.9977388	76.96	7816.43	7.5852	345.7559	90.042
112	.9977335	77.14	7893.58	7.8382	353.5941	90.047
113	.9977282	77.32	7970.90	8.1068	361.7008	90.053
114	.9977229	77.50	8048.40	8.3925	370.0933	90.060
115	.9977175	77.69	8126.09	8.6967	378.7901	90.068
116	.9977121	77.87	8203.96	9.0214	387.8115	90.076
117	.9977066	78.06	8282.02	9.3684	397.1799	90.086
118	.9977010	78.25	8360.27	9.7400	406.9199	90.096
119	.9976955	78.44	8438.71	10.1388	417.0587	90.107
120	.9976898	78.63	8517.34	5.2838	422.3425	90.119

APOGEE BURNS

BURN NUMBER	MASS RATIO	DELV BURN	DELV TOT	THIS TIME	TOTAL TIME	PROP BURN
1	.9856745	475.63	475.63	11.0119	11.0119	557.541
2	.9856343	476.97	952.60	11.5169	22.5288	551.096
3	.9855673	479.21	1431.82	12.0914	34.6202	545.712
4	.9854735	482.35	1914.17	12.7467	47.3669	541.330
5	.9853530	486.38	2400.55	13.4971	60.8640	537.893
6	.9852057	491.31	2891.86	14.3608	75.2247	535.345
7	.9850316	497.13	3388.99	15.3616	90.5863	533.630
8	.9848308	503.85	3892.85	16.5308	107.1171	532.694
9	.9846033	511.47	4404.32	17.9100	125.0271	532.482
10	.9843491	519.98	4924.30	19.5561	144.5832	532.940
11	.9840682	529.39	5453.69	21.5482	166.1314	534.015
12	.9837606	539.70	5993.39	.0000	166.1314	535.653

******** MULTIBURN OUTPUT SUMMARY ***********

****** ROCKET MASS SUMMARY ******

GROSS IGNITION WEIGHT (LBM) = 50000.00
DRY MASS DELIVERED GEO (LBM) = 31849.34
PROPELLANT MASS BURNED (LBM) = 18332.17
VEHICLE INERT WEIGHT (LBM) = 3257.78
DELIVERED PAYLOAD (LBM) = 28410.04
WTHRST = 474.1
WREF SYS = 598.8
WFEED = 1760.

****** ROCKET PERF SUMMARY *******

PROPELLANT MASS FRACTION = .849106
ROCKET VACUUM THRUST (LBF) = 50.79
SPECIFIC IMPULSE (SEC) = 1000.000
MAXIMUM ACCELERATION (G) = .001595
MINIMUM ACCELERATION (G) = .001016
NUMBER OF PERIGEE BURNS = 120
NUMBER OF APOGEE BURNS = 12
RNORM = 15.90
POWIN = 2.2156E+06

****** ORBITAL INFORMATION *******

INITIAL ORBIT

INITIAL ORBITAL ALT (NMI) = 150.00
INITIAL ORBIT RADIUS (NMI) = 3593.92
INITIAL ORBIT PERIOD (HRS) = 1.5011
INITIAL ORBIT VELOCITY (FPS) = 25389.23

TRANSFER ORBIT

ORBITAL PERIOD (HRS) = 10.5676
PERIGEE VELOCITY (FPS) = 33372.62
APOGEE VELOCITY (FPS) = 5258.63

FINAL ORBIT

APPENDIX B

MODIFIED MULTIBURN RESULTS

TOTAL TIMES SPENT AT A GIVEN ALTITUDE INTERVAL

```
**************** FINAL ALTITUDE AND TIME DATA
ALTITUDE INTERVAL(KM)      AND          TIME AT THAT INTERVAL (MINUTES)
 200   TO   400         TIME(MINS):   1542.
 400   TO   600         TIME(MINS):   1024.
 600   TO   800         TIME(MINS):   735.9
 800   TO   1000        TIME(MINS):   628.1
 1000  TO   1200        TIME(MINS):   474.0
 1200  TO   1400        TIME(MINS):   495.2
 1400  TO   1600        TIME(MINS):   433.6
 1600  TO   1800        TIME(MINS):   392.6
 1800  TO   2000        TIME(MINS):   405.3
 2000  TO   2200        TIME(MINS):   335.5
 2200  TO   2400        TIME(MINS):   327.3
 2400  TO   2600        TIME(MINS):   352.5
 2600  TO   2800        TIME(MINS):   327.6
 2800  TO   3000        TIME(MINS):   282.0
 3000  TO   3200        TIME(MINS):   277.5
 3200  TO   3400        TIME(MINS):   297.6
 3400  TO   3600        TIME(MINS):   275.7
 3600  TO   3800        TIME(MINS):   322.7
 3800  TO   4000        TIME(MINS):   245.7
 4000  TO   4200        TIME(MINS):   223.7
 4200  TO   4400        TIME(MINS):   252.1
 4400  TO   4600        TIME(MINS):   241.8
 4600  TO   4800        TIME(MINS):   241.9
 4800  TO   5000        TIME(MINS):   260.0
 5000  TO   5200        TIME(MINS):   251.1
 5200  TO   5400        TIME(MINS):   178.7
 5400  TO   5600        TIME(MINS):   221.5
 5600  TO   5800        TIME(MINS):   220.0
 5800  TO   6000        TIME(MINS):   225.4
 6000  TO   6200        TIME(MINS):   213.7
 6200  TO   6400        TIME(MINS):   183.6
 6400  TO   6600        TIME(MINS):   241.8
 6600  TO   6800        TIME(MINS):   222.6
 6800  TO   7000        TIME(MINS):   181.0
 7000  TO   7200        TIME(MINS):   199.9
 7200  TO   7400        TIME(MINS):   166.6
 7400  TO   7600        TIME(MINS):   195.4
 7600  TO   7800        TIME(MINS):   221.5
 7800  TO   8000        TIME(MINS):   152.3
 8000  TO   8200        TIME(MINS):   198.2
 8200  TO   8400        TIME(MINS):   164.9
 8400  TO   8600        TIME(MINS):   173.3
 8600  TO   8800        TIME(MINS):   187.4
 8800  TO   9000        TIME(MINS):   211.5
 9000  TO   9200        TIME(MINS):   193.6
 9200  TO   9400        TIME(MINS):   159.0
 9400  TO   9600        TIME(MINS):   163.9
 9600  TO   9800        TIME(MINS):   160.4
 9800  TO   10000       TIME(MINS):   116.6

 10000 TO   10200         TIME(MINS):   173.4
 10200 TO   10400         TIME(MINS):   160.9
 10400 TO   10600         TIME(MINS):   164.9
 10600 TO   10800         TIME(MINS):   186.0
 10800 TO   11000         TIME(MINS):   150.0
 11000 TO   11200         TIME(MINS):   195.1
 11200 TO   11400         TIME(MINS):   182.0
 11400 TO   11600         TIME(MINS):   187.5
 11600 TO   11800         TIME(MINS):   131.7
 11800 TO   12000         TIME(MINS):   122.9
 12000 TO   12200         TIME(MINS):   191.5
 12200 TO   12400         TIME(MINS):   138.8
 12400 TO   12600         TIME(MINS):   110.5
```

66	12600	TO	12800	TIME(MINS):	116.9
67	12800	TO	13000	TIME(MINS):	146.8
68	13000	TO	13200	TIME(MINS):	155.7
69	13200	TO	13400	TIME(MINS):	111.3
70	13400	TO	13600	TIME(MINS):	206.4
71	13600	TO	13800	TIME(MINS):	132.0
72	13800	TO	14000	TIME(MINS):	125.8
73	14000	TO	14200	TIME(MINS):	190.0
74	14200	TO	14400	TIME(MINS):	178.2
75	14400	TO	14600	TIME(MINS):	125.4
76	14600	TO	14800	TIME(MINS):	134.8
77	14800	TO	15000	TIME(MINS):	181.1
78	15000	TO	15200	TIME(MINS):	141.9
79	15200	TO	15400	TIME(MINS):	56.90
80	15400	TO	15600	TIME(MINS):	199.8
81	15600	TO	15800	TIME(MINS):	106.1
82	15800	TO	16000	TIME(MINS):	194.9
83	16000	TO	16200	TIME(MINS):	30.34
84	16200	TO	16400	TIME(MINS):	221.7
85	16400	TO	16600	TIME(MINS):	45.06
86	16600	TO	16800	TIME(MINS):	91.85
87	16800	TO	17000	TIME(MINS):	147.7
88	17000	TO	17200	TIME(MINS):	124.8
89	17200	TO	17400	TIME(MINS):	164.5
90	17400	TO	17600	TIME(MINS):	172.7
91	17600	TO	17800	TIME(MINS):	125.7
92	17800	TO	18000	TIME(MINS):	80.86
93	18000	TO	18200	TIME(MINS):	125.1
94	18200	TO	18400	TIME(MINS):	215.4
95	18400	TO	18600	TIME(MINS):	84.92
96	18600	TO	18800	TIME(MINS):	267.3
97	18800	TO	19000	TIME(MINS):	54.87
98	19000	TO	19200	TIME(MINS):	55.55
99	19200	TO	19400	TIME(MINS):	175.0
100	19400	TO	19600	TIME(MINS):	56.91
101	19600	TO	19800	TIME(MINS):	118.5
102	19800	TO	20000	TIME(MINS):	197.3
103	20000	TO	20200	TIME(MINS):	36.35
104	20200	TO	20400	TIME(MINS):	103.7
105	20400	TO	20600	TIME(MINS):	194.6
106	20600	TO	20800	TIME(MINS):	.0000
107	20800	TO	21000	TIME(MINS):	165.4
108	21000	TO	21200	TIME(MINS):	197.2
109	21200	TO	21400	TIME(MINS):	80.52
110	21400	TO	21600	TIME(MINS):	170.6
111	21600	TO	21800	TIME(MINS):	162.2
112	21800	TO	22000	TIME(MINS):	54.24
113	22000	TO	22200	TIME(MINS):	177.5
114	22200	TO	22400	TIME(MINS):	104.7
115	22400	TO	22600	TIME(MINS):	43.01
116	22600	TO	22800	TIME(MINS):	233.2
117	22800	TO	23000	TIME(MINS):	98.20
118	23000	TO	23200	TIME(MINS):	109.4
119	23200	TO	23400	TIME(MINS):	74.89
120	23400	TO	23600	TIME(MINS):	118.9
121	23600	TO	23800	TIME(MINS):	180.2
122	23800	TO	24000	TIME(MINS):	105.6
123	24000	TO	24200	TIME(MINS):	156.4
124	24200	TO	24400	TIME(MINS):	.0000
125	24400	TO	24600	TIME(MINS):	166.8
126	24600	TO	24800	TIME(MINS):	33.94
127	24800	TO	25000	TIME(MINS):	134.8
128	25000	TO	25200	TIME(MINS):	126.1
129	25200	TO	25400	TIME(MINS):	173.1
130	25400	TO	25600	TIME(MINS):	171.3

APPENDIX C

SPATIAL DENSITIES

(Dr. D.S. Mc Knight)

Debris Samptings for Satellites

Band (km)	No. Objects	Obj hr/day	Spatial Density (obj/cu km)
0 to 50	1	1.606929	0.2599062456941053E-11
50 to 100	4	3.126543	0.4978840550166816E-11
100 to 150	19	8.267196	0.1296337336934861E-10
150 to 200	65	147.6135	0.2279467036104500E-09
200 to 250	138	174.9145	0.2660302029101430E-09
250 to 300	252	411.5040	0.6164911281471052E-09
300 to 350	344	1087.587	0.1605142005971773E-08
350 to 400	428	1065/965	0.1550021681088194E-08
400 to 450	552	1676.408	0.2401967343189206E-08
450 to 500	690	2213.975	0.3126077852603632E-08
500 to 550	1026	3188.870	0.4437616827217346E-08
550 to 600	1334	4151.545	0.5694480678043083E-08
600 to 650	1574	5806.203	0.7850782926742040E-08
650 to 700	1721	5564.284	0.7417382664650155E-08
700 to 750	1842	6189.738	0.8135382156671757E-08
750 to 800	2257	10466.65	0.1356502874878124E-07
800 to 850	2325	9163.976	0.1171242144870846E-07
850 to 900	2237	7757.214	0.9776967297505460E-08
900 to 950	2309	7845.704	0.9754818824792728E-08
950 to 1000	2588	12797.74	0.1558579959154532E-07
1000 to 1050	2360	7361.207	0.8906840929941927E-08
1050 to 1100	2069	5537.271	0.6610339983129161E-08
1100 to 1150	1864	2972.150	0.3500993347246819E-08
1150 to 1200	1722	2419.010	0.2811831303721698E-08
1200 to 1250	1637	1681.589	0.1929037614608955E-08
1250 to 1300	1628	2127.983	0.2409326090255036E-08
1300 to 1350	1651	1904.722	0.2128642127092016E-08
1350 to 1400	1725	2608.485	0.2877662584286514E-08
1400 to 1450	1961	5441.608	0.5926458285249746E-08
1450 to 1500	2207	8900.669	0.9570679535567579E-08
1500 to 1550	1935	4855.020	0.5154641935063285E-08

Debris Samplings for Satellites (Continued)

Band (km)	No. Objects	Obj hr/day	Spatial Density (obj/cu km)
1550 to 1600	1721	2395.986	0.2511967004175655E-08
1600 to 1650	1603	1760.118	0.1822333409955099E-08
1650 to 1700	1524	1626.569	0.1663216476889449E-08
1700 to 1750	1415	1141.005	0.1152359437392957E-08
1750 to 1800	1341	913.4477	0.9112568714450620E-09
1800 to 1850	1270	760.1544	0.7491150628152655E-09
1850 to 1900	1219	667.5206	0.6498800420394691E-09
1900 to 1950	1170	584.1207	0.5618558241441207E-09
1950 to 2000	1134	541.4126	0.5145607186040955E-09
2000 to 2050	1093	535.1542	0.5025771598361100E-09
2050 to 2100	1048	493.4404	0.4579368856310043E-09
2100 to 2150	973	362.0212	0.3320338952900740E-09
2150 to 2200	907	233.6187	0.2117695391357762E-09
2200 to 2250	877	174.9677	0.1567656950509192E-09
2250 to 2300	869	160.5325	0.1421748141901380E-09
2300 to 2350	856	134.6452	0.1178815884591715E-09
2350 to 2400	852	124.5987	0.1078432372894129E-09
2400 to 2450	849	125.4796	0.1073754485770044E-09
2450 to 2500	846	120.8707	0.1022665678956541E-09
2500 to 2550	840	100.6126	0.8417305210199332E-09
2550 to 2600	837	94.76492	0.7839782985182263E-09
2600 to 2650	835	96.89417	0.7927145790290852E-09
2650 to 2700	834	90.23243	0.7300816296625897E-09
2700 to 2750	832	85.59013	0.6849336740589221E-09
2750 to 2800	844	188.2970	0.1490426371665348E-09
2800 to 2850	838	101.4034	0.7939402678987912E-10
2850 to 2900	837	89.19577	0.6908333493569969E-10
2900 to 2950	840	85.44997	0.6547267688838157E-10
2950 to 3000	844	80.81250	0.6125915475806957E-10
3000 to 3050	843	76.78901	0.5758572201360424E-10
3050 to 3100	846	81.87234	0.6075644637405624E-10

Debris Samplings for Satellites (Continued)

Band (km)	No. Objects	Obj hr/day	Spatial Density (obj/cu km)
3100 to 3150	849	85.61419	0.6286643900307874E-10
3150 to 3200	851	88.00147	0.6394477078822938E-10
3200 to 3250	855	89.45557	0.6432625671789372E-10
3250 to 3300	858	88.06644	0.6267301979278323E-10
3300 to 3350	863	105.8137	0.7452893280968370E-10
3350 to 3400	862	118.4621	0.8258435679102947E-10
3400 to 3450	866	124.4817	0.8589788677873132E-10
3450 to 3500	863	112.3143	0.7671728644880264E-10
3500 to 3550	867	130.3320	0.8812772070344463E-10
3550 to 3600	870	130.5947	0.8742043083044551E-10
3600 to 3650	872	165.4352	0.1096384038516520E-09
3650 to 3700	883	306.4097	0.2010511627158161E-09
3700 to 3750	882	235.7542	0.1531630885711374E-09
3750 to 3800	868	122.2742	0.7865774564548039E-10
3800 to 3850	861	112.1764	0.7145644318044893E-10
3850 to 3900	859	104.9593	0.6620861815572869E-10
3900 to 3950	856	110.7757	0.6920109823800033E-10
3950 to 4000	849	80.18132	0.4960627223005597E-10
4000 to 4050	845	73.74618	0.4518748834388251E-10
4050 to 4100	841	72.88008	0.4423060674991847E-10
4100 to 4150	840	67.09614	0.4033358334382498E-10
4150 to 4200	841	72.17503	0.4297651528475500E-10
4200 to 4250	841	98.96992	0.5837701197205649E-10
4250 to 4300	838	88.89803	0.5194508582761376E-10
4300 to 4350	833	61.86168	0.3581021451482455E-10

APPENDIX D

DIFFERENT CONTOUR PLOT ATTEMPTS (ALT vs INCLINATION)

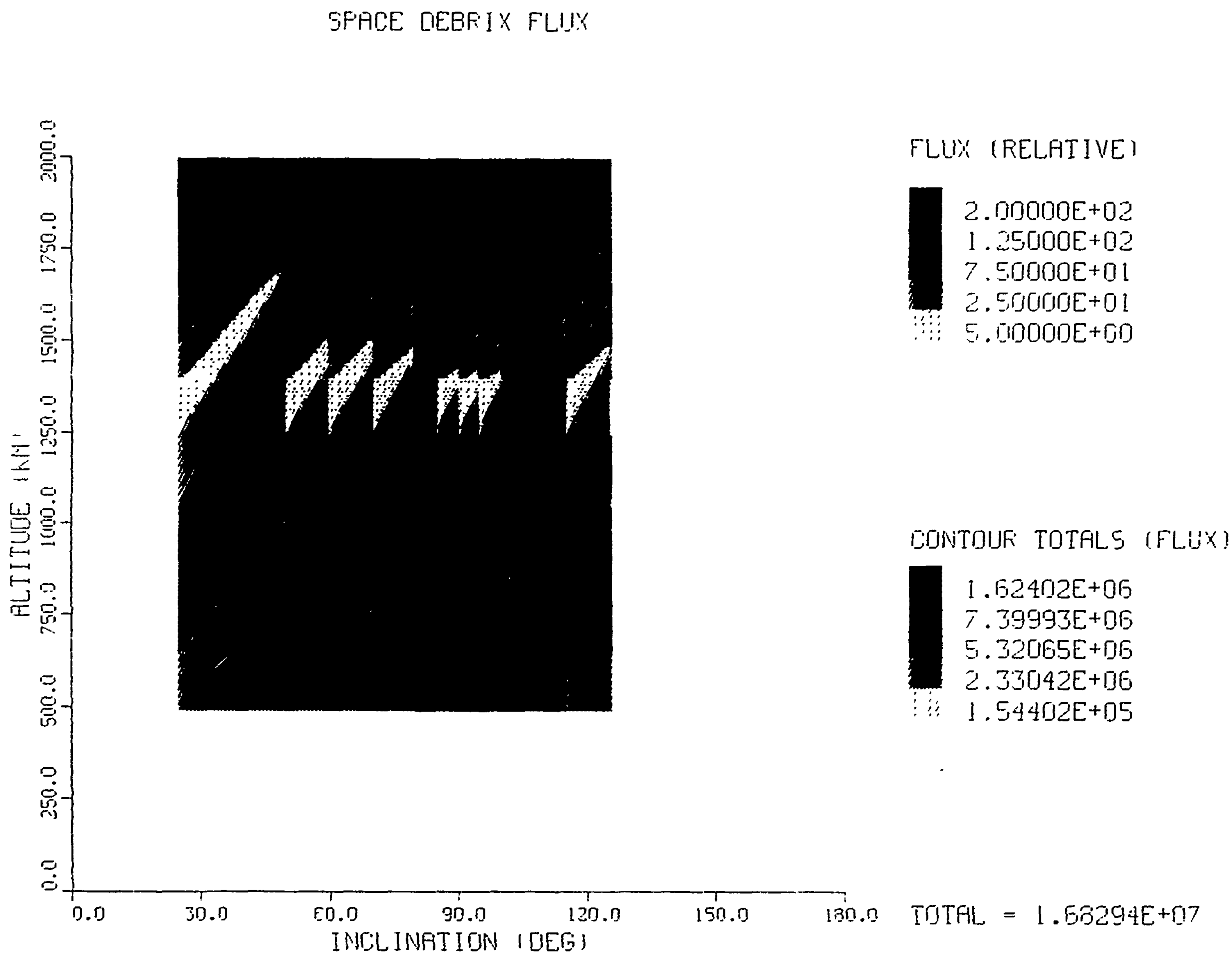
SPACE DEBRIX FLUX
ALTITUDE (KM)
0.0
250.0
500.0
750.0
1000.0
1250.0
1500.0
1750.0
2000.0
INCLINATION (DEG)
0.0
30.0
60.0
90.0
120.0
150.0
180.0
FLUX (RELATIVE)
2.00000E+02
1.25000E+02
7.50000E+01
2.50000E+01
5.00000E+00
CONTOUR TOTALS (FLUX)
1.62402E+06
7.39993E+06
5.32065E+06
2.33042E+06
1.54402E+05
TOTAL = 1.68294E+07

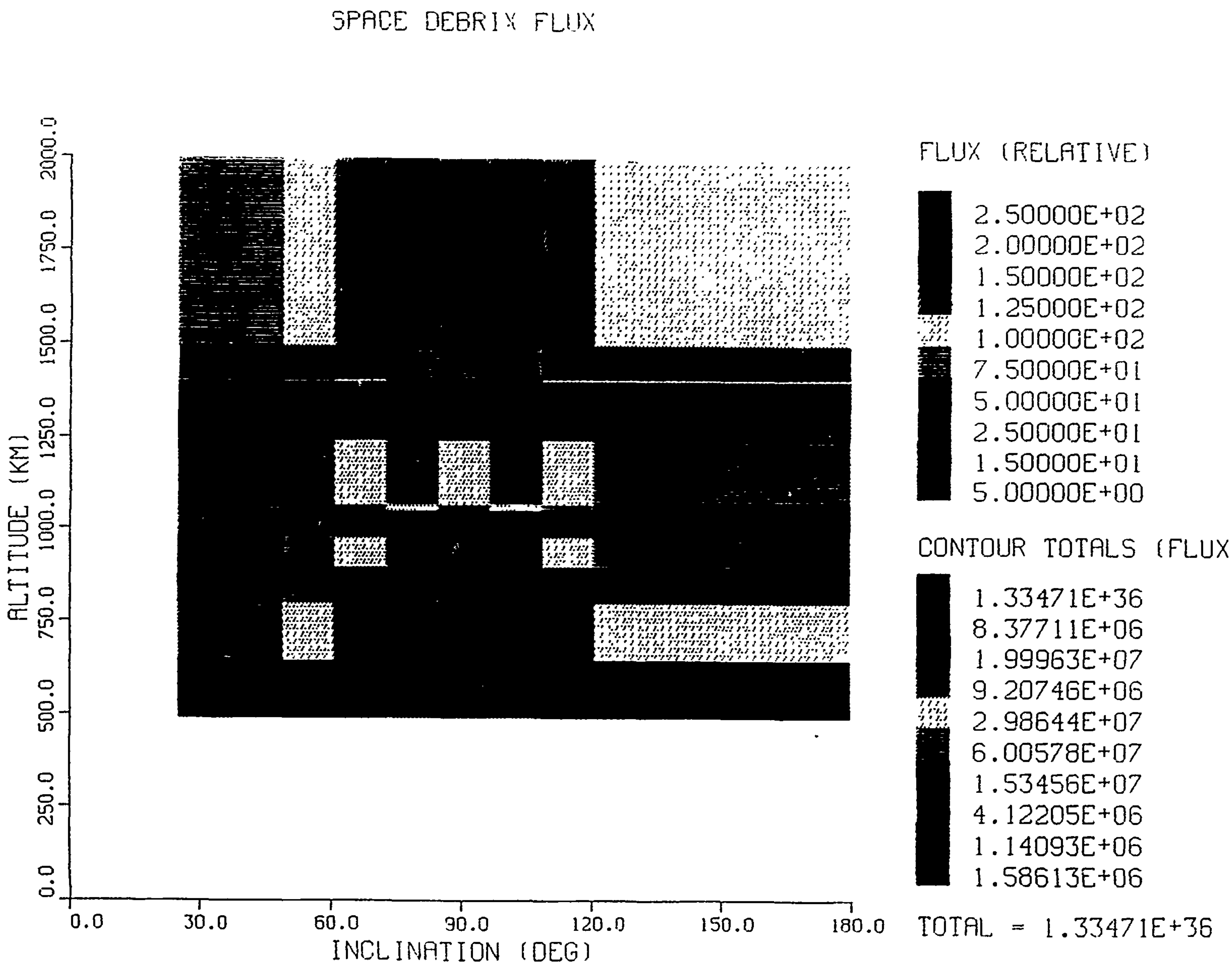
SPACE DEBRIX FLUX
ALTITUDE (KM)
0.0
250.0
500.0
750.0
1000.0
1250.0
1500.0
1750.0
2000.0
INCLINATION (DEG)
0.0
30.0
60.0
90.0
120.0
150.0
180.0
FLUX (RELATIVE)
2.50000E+02
2.00000E+02
1.50000E+02
1.25000E+02
1.00000E+02
7.50000E+01
5.00000E+01
2.50000E+01
1.50000E+01
5.00000E+00
CONTOUR TOTALS (FLUX)
1.33471E+36
8.37711E+06
1.99963E+07
9.20746E+06
2.98644E+07
6.00578E+07
1.53456E+07
4.12205E+06
1.14093E+06
1.58613E+06
TOTAL = 1.33471E+36

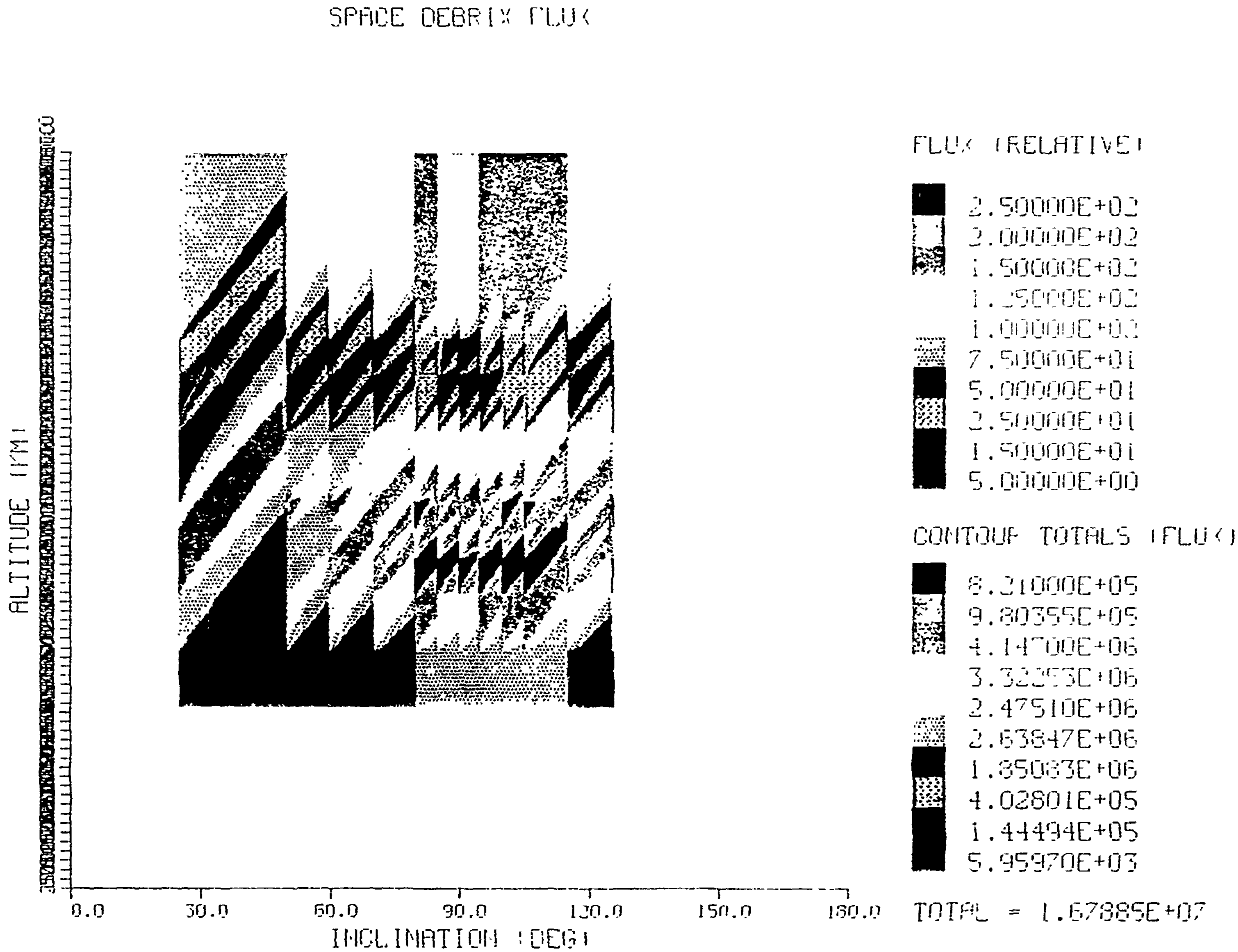
SPACE DEBRIS FLUX
ALTITUDE (KM)
0.0
30.0
60.0
90.0
120.0
150.0
180.0
INCLINATION (DEG)
FLUX (RELATIVE)
2.50000E+02
2.00000E+02
1.50000E+02
1.25000E+02
1.00000E+02
7.50000E+01
5.00000E+01
2.50000E+01
1.50000E+01
5.00000E+00
CONTOUR TOTALS (FLUX)
8.21000E+05
9.80355E+05
4.14700E+06
2.47510E+06
2.63847E+06
1.85083E+06
4.02801E+05
1.44494E+05
5.95970E+03
TOTAL = 1.67885E+07

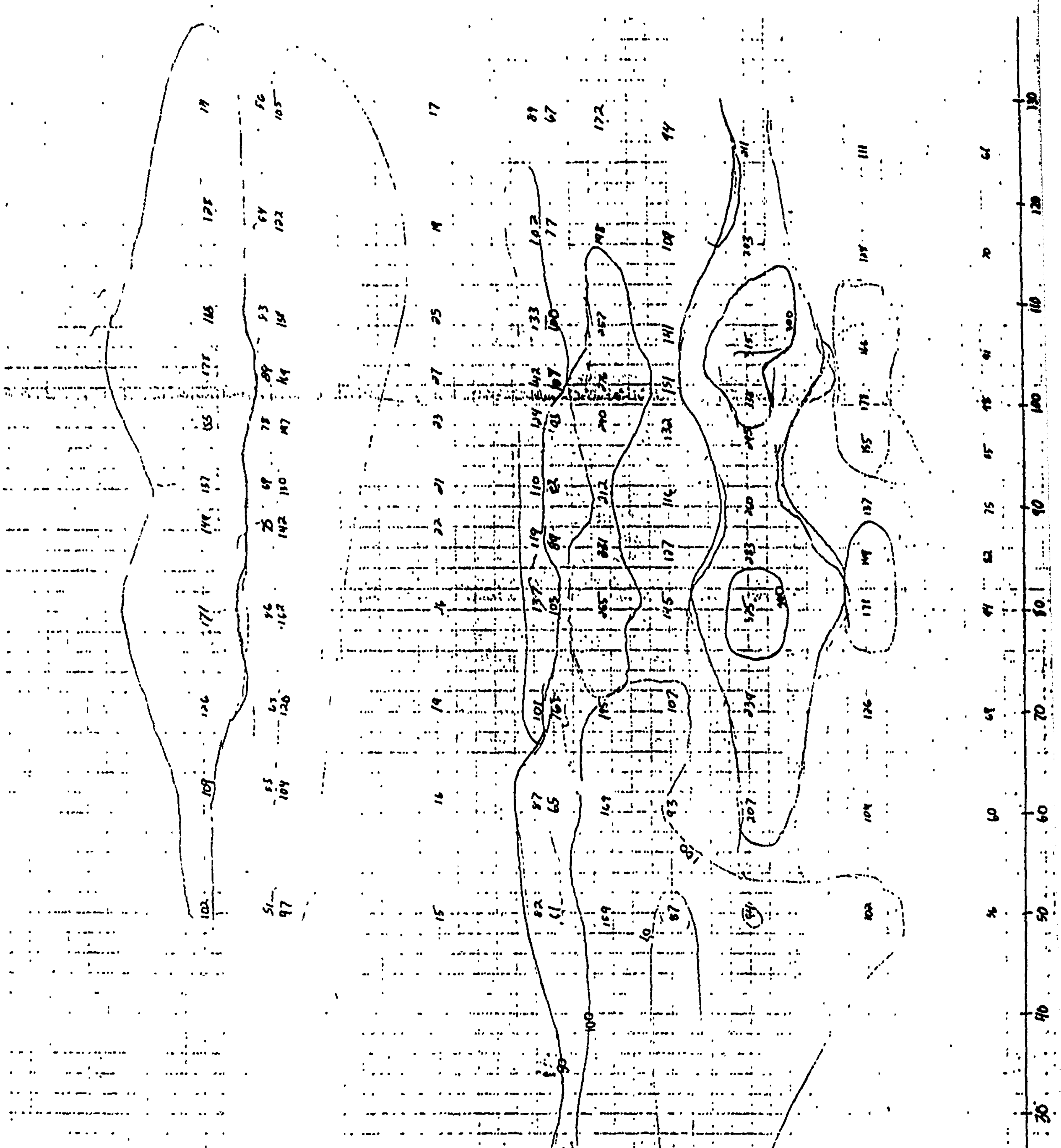
HEIGHT (KM)